http://ansinet.com/itj

ITJ

ISSN 1812-5638

INFORMATION TECHNOLOGY JOURNAL

ANSInet
Asian Network for Scientific Information
308 Lasani Town, Sargodha Road, Faisalabad - Pakistan

Information Technology Journal 12 (7): 1350-1357, 2013
ISSN 1812-5638 / DOI: 10.3923/itj.2013.1350.1357

Segmentation Algorithms for Non-uniform Froth Image Based on Adaptive Morphology

[1,2]Jianqi Li, [1]Chunhua Yang, [1]Hongqiu Zhu, [1]Jinping Liu and [1]Binfang Cao
[1]College of Information Science and Engineering, Central South University, Changsha, China
[2]School of Communication and Electric Engineering, Hunan University of Arts and Science Chang de, China

Abstract: Feature parameters of froth image in flotation process are closely associated with the industrial situations. This study has presented an improved watershed algorithm based on adaptive morphological operation, considering lack of background and various non-uniform froths conglutinating together. Firstly, Two-Dimensional Histogram Minimum Cross-Entropy (GLCM) is used to estimate the froth distribution, which is divided into three regions: large, middle and small. Secondly, the image is enhanced by multi-scale Retinex algorithm, due to the effects imposed by light and noises. Then, the optimal structural element is used to perform morphological filtering according to regions types and extract mark points using adaptive area morphology reconstruction. Lastly, results are obtained through watershed algorithm. Simulation indicated that proposed algorithm is more robust in segmenting unevenly-distributed froth image, overcoming over-segmentation and under-segmentation effectively.

Key words: Flotation froth, image segmentation, multi-scale retinex algorithm, self-adaptive mathematical morphology, watershed algorithm

INTRODUCTION

Flotation of minerals is to improve grade of raw minerals, reagent is added to generate a kind of froth with stable property. By collecting mineral ores with froth inside, it reveals the close correlation between shapes of froth and process parameters (Moolman *et al*., 1996; Sadr-Kazemi and Cilliers, 1997). Segmentation of froth image aims at seeking out crucial methods to extract features but image is usually covered by froth (Hyotyniemi and Ylinen, 2000). Uneven lightness, irregular shapes and conglutination between complicated contours make it more difficult to segment (Aldrich *et al*., 2010). Conventional segmentation algorithm was successful in detecting some of brighter spots but missing out important information on contours (Wang *et al*., 2003). Considering the inferior quality of detection and uneven gray value uniformity of froths, plenty of algorithms have been proposed, histogram threshold, morphology, valley edge tracking and watershed (Wang, 1998; Lin *et al*., 2008; Marais and Aldrich, 2011). But watershed algorithm is more suitable in segmenting froth image. Improved watershed algorithm proposed by Yang *et al*. (2008, 2009) has been successful in extracting watershed marks but parameters on spot largely depends on real-time images. Adaptive segmentation algorithm proposed by Zhou *et al*. (2010) segments the image roughly, firstly extracts and recognizes local textures, then finely segments local regions or merges regions. However, calculation is more complicated and texture is unstable. Only in segmenting froth images of uniform shapes, these algorithms had good effect but in segmenting conglutinate images over-segmentation is commonly seen.

Three shapes of froths can be roughly classified, small, medium and large respectively (Zhou *et al*., 2010). Fixed structural element is often used to pre-process because lots of froths mixing together, which is improper under complicated industrial conditions. Structural elements weigh heavily important in morphological filtering but if greater element the smaller froths are missing and noises cannot be removed. Existing area reconstruction algorithms have synthesized fixed area parameters to extract marked points on whole image-important way to overcome over-segmentation but needs to be optimized. Existing studies fail to process the situation when there is uneven light distribution, which merely use singular structural element to process the mingled non-uniform froth image. In this case, mark points and contour of froth are unable to be obtained precisely. Even worse, the false segmentation of froth image often causes difficulties in extracting the feature parameters, which severely affects the process in industrial control and optimization.

Corresponding Author: Chunhua Yang, College of Information Science and Engineering, Central South University, Changsha, China

ALGORITHM PRINCIPLE

This study has presented adaptive mathematical morphology, especially for uneven froth images, concrete flow shown in Fig. 1. Multi-scale Retinex was introduced to enhance lightness uniformity that were lessened by exposing to industrial illumination. Bright points on image reflected the sizes and shapes (Yang *et al*., 2008) of froths but noises occurred frequently because of highly concentrated pixel value. In this article, two-dimensional local cross-entropy threshold was adopted to segment bright points, estimate morphological characteristics and to classify regions. Then pre-processed the image using optimized structural elements according to froth types. Meanwhile, improved adaptive area reconstruction was employed to extract marked points (local minimum of morphology gradient image). Finally, segmented gradient image using improved watershed algorithm to obtain the image with better robustness.

Two-dimensional local cross-entropy threshold based on gray-level co-occurrence matrix: Threshold algorithm is a parallel regional segmentation technique to directly extract object. With flotation of froth image, brighter points are be rapidly extracted using the algorithm. By analyzing the number of brighter points, the size and shape of froths can be estimated out. Regions can be classified when brighter points are known, which is a foundation for adaptive morphology and extraction of marked points.

On part of probability and information theory, cross-entropy is to measure gray errors between the segmented image and the original one. But in most cases, only the information of gray value is useful to threshold image. Spatial structural information was not used but very important in froth image where histogram displays single peak, 95% pixels between 150 and 200. Gray Level Co-occurrence Matrix (GLCM) is defined by joint probability density of pixels in two different locations, not only represents how brightness is distributed but distribution characteristics of pixels of the same or similar brightness. Gray level Co-occurrence Matrix reflects the second-order statistics property of brightness when it is changing. It is a good way to tap the secret of image's distributive property (Nie *et al*., 2011).

Suppose froth image f (x, y), size M×N, gray level L. GLCM (L×L) is shown in Fig. 2. $W = [t_{ij}]_{L\times L}$, where t_{ij} is the value of ith element in matrix. Normalization of GLCM

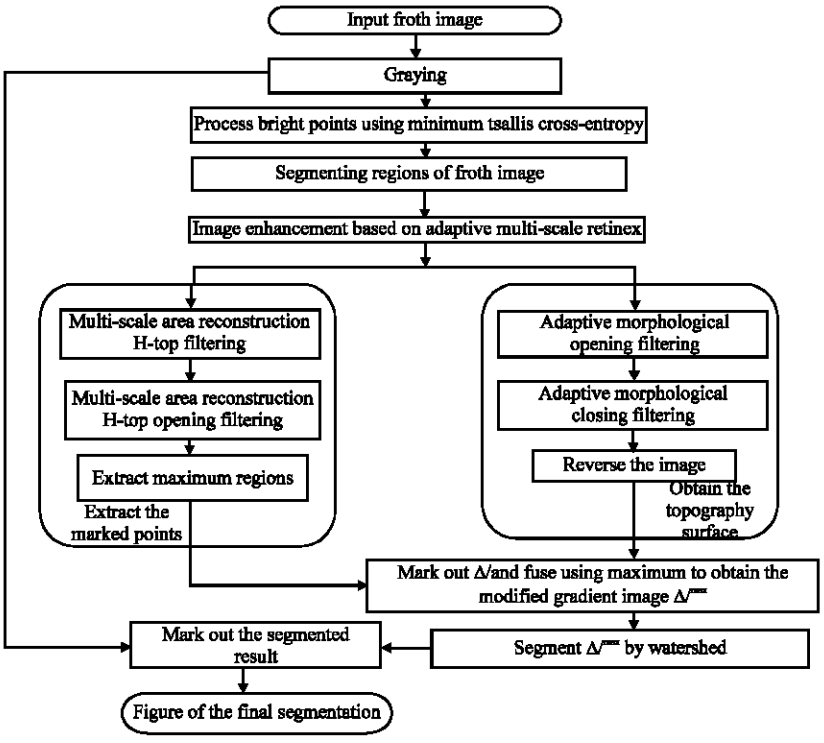

Fig. 1: Diagram of improved algorithm

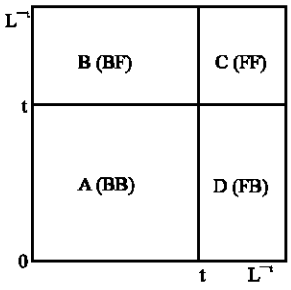

Fig. 2: Image Gray-GLCM matrix

generates the transfer probability of gray level from i to j-GLCM can be defined in Eq. 1:

$$t_{ij} = \sum_{m=1}^{M}\sum_{n=1}^{N}\delta_{mn}$$

$$\delta_{mn} = 1 \quad \text{if} \begin{cases} f(m,n) = i \ \text{and} f(m+1,n) = j \\ \text{and/or} \\ f(m,n) = i \ \text{and} f(m,n+1) = j \end{cases} \qquad (1)$$

$$= 0; \quad \text{otherwise}$$

In this study, symmetrical reconstruction norms of threshold algorithm based on cross-entropy has been used. Cross-entry is expounded as J (A|B)= D (A|B)+D (B|A). Suppose t represents the optimal segmentation threshold value. A and B characterize the probability of characteristics vector of pixels in the bright and background regions. Calculate the optimal threshold value to minimize information difference before and after segmentation process. t divides Gray Level Co-occurrence Matrix into four quadrants, A, B, C, D, in Fig. 2.

Suppose pixel value below t is background but above t is foreground. A corresponds to local transform of image background, C corresponds to local transform of image foreground; B and D correspond to joint transform of contour information on background and foreground (Nie *et al*., 2011). Transform probability of four quadrants can be defined from the average value:

$$P_A^t = \sum_{i=0}^{t}\sum_{j=0}^{t} p_{ij}, P_B^t = \sum_{i=0}^{t}\sum_{j=t+1}^{L-1} p_{ij}$$

$$P_C^t = \sum_{i=t+1}^{L-1}\sum_{j=t+1}^{L-1} p_{ij}, P_D^t = \sum_{i=t+1}^{L-1}\sum_{j=0}^{L-1} p_{ij} \qquad (2)$$

In the matrix, A and C mainly relate to Background-background (BB) information and Foreground-foreground (FF) local transform information; B and D merely involve Background-foreground (BF) information and Foreground-background (FB) information of the contour transform. Considering information of B and D is so tiny in the whole image, that its proportion can almost be ignored. Methods in this study merely consider the influence of A and C upon optimal threshold value. Suppose μ_A^t, μ_C^t is gray level of A, C, so:

$$\mu_A^t = \frac{1}{P_A^t}\sum_{i=0}^{t}\sum_{j=0}^{t}(ijp_{ij}), \mu_C^t = \frac{1}{P_C^t}\sum_{i=t+1}^{L-1}\sum_{j=t+1}^{L-1}(ijp_{ij}) \qquad (3)$$

Local symmetrical cross-entropy of GLCM quadrant A and C before and after threshold algorithm can be defined as:

$$J(A|t) = \sum_{i=0}^{t}\sum_{j=0}^{t} ijp_{ij}\log\frac{ij}{\mu_A^t} + \sum_{i=0}^{t}\sum_{j=0}^{t}\mu_A^t p_{ij}\log\frac{\mu_A^t}{ij} \qquad (4)$$

$$J(C|t) = \sum_{i=t+1}^{L-1}\sum_{j=t+1}^{L-1} ijp_{ij}\log\frac{ij}{\mu_C^t} + \sum_{i=t+1}^{L-1}\sum_{j=t+1}^{L-1}\mu_C^t p_{ij}\log\frac{\mu_C^t}{ij} \qquad (5)$$

Minimum two-dimensional local cross-entropy norms of threshold can be defined as:

$$J_{LTCE}(t) = J(A|t)+J(C|t) \qquad (6)$$

where, $J_{LTCE}(t)$ describes the cross-entropy of local gray level transform of A and C, reflects how the image processed by threshold value matches with original one. If Eq. 6 as an effective threshold norms, the optimal threshold value can be obtained by Eq. 7:

$$t^* = \arg\min_{t\in G} J_{LTCE}(t) \qquad (7)$$

Classification and marker of froth image: It takes a long time before flotation process is completed but meanwhile little change happens to froth image. Everyday video images are captured two times when industrial conditions turn stabilized. Two images were chosen as experimentation samples, 60 images in total with 4 excluded for their abnormal property. Remaining 56 images were selected as sample bank for further analysis. In experimentation, used two-dimensional local cross-entropy segmentation of GLCM to extract the average value of white bright point, based on which FCM algorithm was applied to perform clustering analysis for sample sets. Clustering analysis showed that white bright points were classified as small-size froth when average value 350; 350-600 they were sorted into middle-size froth average value; above 600 as the large-size bubbles. Classification method had similar effect with human vision. Based on the norm, in this article regions in each image were classified. Region grew on the bright points until all regions have been classified, three types of regions were marked out.

Froth image enhancement based on adaptive multi-scale Retinex algorithm: Equipments used in collecting froth image often include: high-resolution industrial camera, high-frequency light source, etc. Pulp temperature in flotation cell is very high, camera should be installed at a certain distance above the cell to prevent the trapped air from condensing on optic lens. On-spot dust, uneven lightness, non-airtight collecting system where sunlight usually sheds on and little gray value contrast on background between bubbles and pulp, so brightness of froth image is unevenly distributed (Jobson *et al*., 1997). Multi-scale Retinex algorithm has achieved a good effect to improve bright uniformity (Kimmel *et al*., 2003), revealing details in shadowed area.

Retinex algorithm was based on the visual model proposed by Land, to perceive brightness and color. Principles can be explained that image is characterized by multiplying environment brightness function (bright function) and reflection function. Then enhance the image by changing ratio of the reflected image and the bright one. Environment brightness function describes the background intensity and reflection function reflects objects characteristics. Application of Retinex algorithm to enhance on-spot froth image can effectively remove object's background intensity that merely reflects information of the object itself (Jobson *et al*., 1997).

Single-scale Retinex algorithm is described as:

$$R(x,y) = \text{In } I(x,y) - \text{In } [G(x,y) * i(x,y)] \quad (8)$$

$$G(x,y) = \lambda \exp[-\frac{x^2 + y^2}{\varepsilon^2}] \quad (9)$$

where, ε is determined by $\int\int G(x,y)\,dxdy = 1$, dynamic compression is more powerful if smaller ε; color sense uniformity is better if greater ε. To balance dynamic compression and color sense uniformity, use multi-scale Retinex algorithm.

$$R(x,y) = \sum_{i=1}^{k} w_i \{\ln I(x,y) - \ln[G_i(x,y) * I(x,y)\} \quad (10)$$

where, k represents the number of scales, w_i the weight of ith scale ε_k and:

$$\sum_{i=1}^{k} w_i = 1$$

Firstly obtain Peak regions of froth image (bright regions) from section 2.1, then choose 3×2 elliptical structural elements to filter out noises in binary image using gray morphological opening and closing reconstruction filter and smoothing filter. Better region boundary comes out in the way. Next, use Retinex algorithm based on adaptive weight for different regions (Park *et al*., 2008).

Retinex algorithm has used for the large, middle and small scale, k = 3, scale parameter ε_1 = 15, ε_2 = 80 and ε_3 = 200. Weight value w_k adopts regional adaptive value on peak regions, mostly the large, middle scales on smoothing and flat regions (w_1 = 2/5, w_2 = 2/5, w_3 = 1/5).

By analyzing froth image, shown in Fig. 3, there is distinct discrepancy on peaks and edged gray, high-luminous and dark regions, blurring edges and sole pattern of histogram-single peak form where pixels

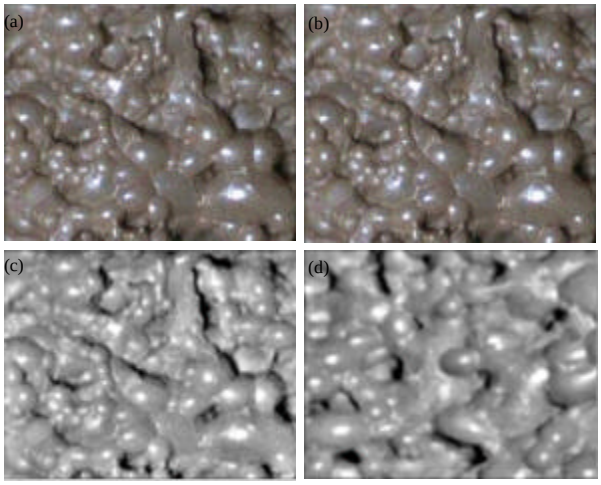

Fig.3(a-d): Process image using improved adaptive MSR (a) Froth image 1, (b) Froth image 2, (c) Processed froth image1 and (d) Processed froth image 2

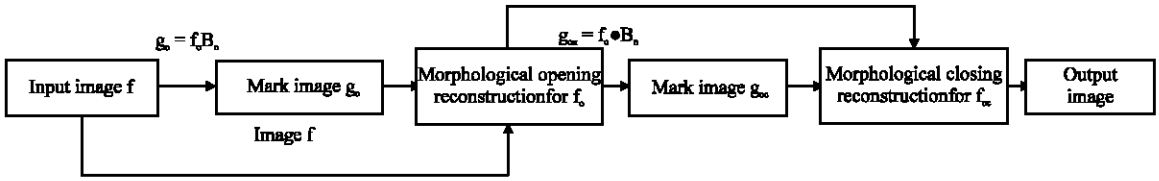

Fig. 4: Adaptive morphological opening and closing reconstruction filter

distribute more densely. Multi-scale Retinex algorithm based on regional adaptive segmentation adjusts weight value to obtain the optimal estimation, so bright uniformity is enhanced. After the processing, regions easily influenced by light are rightly smoothed and there are lesser local minimum regions. Over-segmentation has been effectively reduced, edges are retained, which generating more obvious brightness uniformity.

Adaptive morphological opening and closing reconstruction filtering: Morphological operator retains image as a set. Morphological opening and closing operation is effective in removing the peak points and the isolated islands. Closing operation can fill in holes and gap of images, morphological opening and closing filter is constructed when using these approaches together. Filter not only filters out noises but retains the continuity of object regions-without causing distortion to images. Use three different types of structure elements, B_1, B_2, B_3, to optimize different froth images using optimization algorithm in reference (Yang *et al*., 2008). Concrete flow is shown in Fig. 4:

- f as input mask image; g_o ($g_o = f^{\circ}B_n$) as marked image, output is f_o when using morphological opening operation
- f_o as mask image, g_{oc} ($g_0 = f_o \bullet B_n$) as marked image, output is f_{oc} using morphological closing reconstruction algorithm

The algorithm has good effect in removing dark and bright peak points, noises and retaining the integrity and contour of object information after filtering.

Marked point extraction based on adaptive H-top opening reconstruction transform: Inaccurate segmentation usually happens when using improved watershed algorithm proposed in reference (Yang *et al*., 2008). In this case, in this article improved adaptive marked extraction algorithm has been proposed-adaptive H-top opening reconstruction transform-to extract local minimum. Extract all peak value using improved transform and adopt area threshold value to filter out the area peak whose value is below the specified type. Surrounding environment often effects small details and bright points that generally belong to noises. In addition, merge the neighborhood of low contrast and smaller areas. Morphological Top-hat transform and area reconstruction H-top are applied together to construct adaptive area reconstruction and its improved formula, which provides standards to mark out watershed segmentation points. Top-hat transform operator can be defined as:

$$HAT(f) = f-(f_og) \quad (11)$$

where, "o" represents the opening operation; f the original image. g represents the structural element which selects proper B_n according to region types (Gonzalez and Woods, 2003).

Area reconstruction uses the connected areas as the filtering norms. Morphological reconstruction using gray information not only filters out interference problem but retains geometrical features. In H open reconstruction, the marked image g meets: $\forall p \in D$, $g(p) = f(p)-h$, h specifies a constant. So H opening reconstruction Top-hat transform (H-top opening reconstruction transform) can be defined: $m(p) = f(p)-\rho(p)$, $\rho(p)$ is the result of opening reconstruction. The transform can effectively extract the peak regions according to gray difference h, an accurate guidance for watershed algorithm. H-top opening transform for gray image using adaptive area is defined:

$$\forall p \in D, H(g, h, S) = g(p)-\omega(g, h_n, S_n)(p) \quad (12)$$

where, g (p) represents the gray value of p of g; ω the area reconstruction opening operator, S_n is area threshold value. Corresponding H-top closing operator of area reconstruction can be obtained from its dual characteristics. But improved H-top opening (closing) transform in this article is achieved by following:

- Filtering out regions of smaller area and low contrast using area reconstruction H opening (closing) according to specified parameter h_n and S_n
- Area reconstruction H-top opening (closing) transform for results in Eq. 1

- Non-zero points in Eq. 2 as the output for distinctive regions. Improved opening transform for H-top area reconstruction operates mostly for the bright regions but dual closing operation is designed for darker regions

Top gray value of froth image is relatively greater but on the contour the value is smaller. Every bright point corresponds to one bubble, improved algorithm in the study uses adaptive area reconstruction H-top opening transform to extract mark points of watershed transform and to reverse the froth image. Choose the reversed image as topography surface where watershed line is the contour. Marked points of improved watershed algorithm cannot be known until reverse process has been done for the extracted marked points using H-top adaptive improved area reconstruction H-top opening transform, as shown in Fig. 5.

OBJECTIVE APPRAISAL AND ANALYSIS FOR SEGMENTING FROTH IMAGE

To make a comprehensive comparison towards the affectivity of algorithms, there are two appraisal system, subjective appraisal and objective appraisal, respectively. Subjective appraisal means assessing segmentation from the perspective of human's visual judgment but objective involves taking the froth painted by expert manual workers as the standard output segmentation results. By comparing the similarity between algorithms in the study and the standard segmentation, the appraisal index can be defined as:

$$k = 2 \times \frac{N(M \cap S)}{N(M) + N(S)} \times 100\% \quad (13)$$

where, M and S represent the result of manual segmentation algorithms. M∩S represents the intersection set of M and S, N is the number of pixels in the region (Gonzalez and Woods, 2003).

Some typical froth images were sampled to test, original image was 338*245, as shown in Fig. 6a, 82810 pixels in total. Froth image segmentation algorithm based on valley contour (Yang *et al*., 2009) and improved watershed algorithm (Zhou *et al*., 2010) have been used in the experimentation, shown in Fig. 6b-d. Algorithms have been accomplished using, Intel (R)Core (TM)2 Duo CPU T8100 @2.lOGHz with 2.00GB RAM, Matlabas the programming language. Figure 6b shows the result using valley contour algorithm, 190 bubbles in total. Effect is

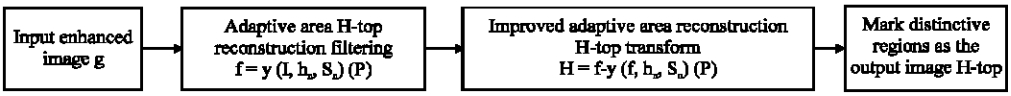

Fig. 5: Diagram flow for extracting adaptive marked points

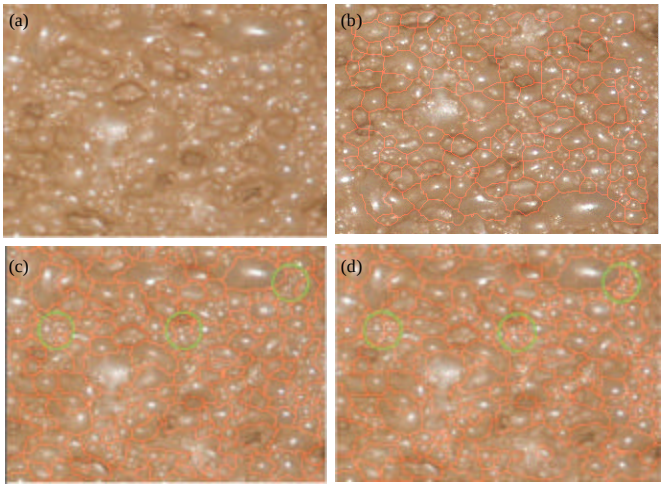

Fig. 6(a-d): Segmentation results using different algorithms (a) Input foam image, (b) Segmentation results with valley edge, (c) Segmentation results and (d) Segmentation results with fixed watershed with adaptive watershed

Table 1: Objective appraisal for different algorithms

Algorithm	Average time (sec)	Average accuracy rate (%)
Valley contour	4.799	86.53
Watershed of fixed parameter	3.985	90.85
Proposed algorithm	3.686	93.98

very common place and over-segmentation is frequently to be found because threshold value to detect valley is time-variant and easily restricted by the size and shape of bubbles. Figure 6c shows the segmentation using watershed algorithm with fixed parameters, 171 bubbles in total. Effect is better and calculation speed has increased apparently but over-segmentation (marked with green) in some smaller regions still exists because of using fixed parameters. Figure 6d shows the results using proposed algorithms in this study, 195 bubbles in total, which has achieved the most desirable segmentation. In actuality, shapes of the segmented results are most approximately the same with bubble. Furthermore, bubbles that adhere to each other are be segmented, shown in green marked points. Compared with the valley contour algorithm and fixed parameter watershed algorithm, proposed algorithm in this article can both segment larges bubbles as well as smaller ones. The segmented image comes nearer to real one.

To reduce the errors caused by manual segmentation, 5 sets of the images are taken as the sample bank. The experiment is conducted with 20 random images from the sample bank and then calculate the operation time and accuracy rates, as shown in Table 1. Compared with (Yang *et al*., 2009), valley contour methods proposed in this study has increased the accuracy by 8%, operation time has declined by 21%, while for the improved watershed algorithm (Zhou *et al*., 2010), the accuracy rate of watershed algorithm boosted by 3.4% and operation time decreased by 5%. The three algorithms have similar effects in segmenting uniform froth image but when industrial conditions are unstable, methods proposed in this study are more accurate. Researchers indicate that the increase of accuracy rate might derive from reducing light and optimizing and classifying the froth regions. But on-spot industrial situation needs real-time operation, so Table 1 has presented a comparison among the three types of algorithms. Methods in Yang *et al*. (2009) requires global optimal templates and Zhou *et al*. (2010) needs improved watershed algorithm to search global structural element. These processes not only consume plenty of time but make it harder to obtain the optimal parameters. Improved algorithms in this study avoids the optimal searching by using regional adaptive methods and saves lots of time. However, Multi-scale Retinex leads to some certain consumption, which consumes approximately amount of time with watershed algorithm by Zhou *et al*. (2010) where light is not removed. In conclusion, algorithms proposed in the study are very applicable in extracting features of froth image in flotation process and in analyzing industrial conditions, with stronger robustness.

CONCLUSION

The study has presented an improved adaptive morphological watershed segmentation algorithm for froth image which extracts bright regions using minimum cross-entropy algorithm, divides and classifies regions according to the shapes of bubbles so that appropriate structural element can be chosen out. Improved algorithm chooses appropriate threshold value to pre-process the image and adaptive area reconstruction to extract the marked points. Based on subjective and objective appraisal, segmented results given by proposed algorithms is applicable mineral froth image and segmenting the image rapidly and accurately. Even though bubbles of different shapes and sizes frequently mix together, the shape can be located, which makes it manageable to control the flotation process. However, it can been seen from these figures, segmentation needs further analysis in areas where bubbles are conglutinated and superimposed together and in special regions where some froths fall through.

ACKNOWLEDGMENTS

This study was supported by the National Science Foundation of China under Grant No. (61134006,61071176), supported by Hunan Province Natural Science Foundation under Grant No. 11JJ6062, respectively.

REFERENCES

Aldrich, C., C. Marais, B.J. Shean and J.J. Cilliers, 2010. Online monitoring and control of froth flotation systems with machine vision: A review. Int. J. Miner. Process., 96: 1-13.

Gonzalez, R.C. and R.E. Woods, 2003. Digital Image Processing. Publishing House of Electronics Industry, Beijing, China.

Hyotyniemi, H. and R. Ylinen, 2000. Modeling of visual flotation froth data. Control Eng. Pract., 3: 313-318.

Jobson, D.J., Z. Rahman and G.A. Woodell, 1997. Properties and performance of a center/surround retinex. IEEE Trans. Image Proc., 6: 451-462.

Kimmel. R., M. Elad, D. Shaked, R. Keshet and I. Sobel, 2003. A variational framework for retinex. Int. J. Comput. Vis., 52: 7-23.

Lin, B., B. Reche, J.K.H. Knudsen and S.B. Jorgensen, 2008. Bubble size estimation for flotation processes. Miner. Eng., 21: 539-548.

Marais C. and C. Aldrich, 2011. Estimation of platinum flotation grades from froth image data. Miner. Eng., 24: 433-441.

Moolman, D.W., C. Aldrich, G.P.J. Schmitz and J.S.J. Van Deventer, 1996. The interrelationship between surface froth characteristics and industrial flotation performance. Miner. Eng., 9: 837-854.

Nie, F., C. Gao, Y. Guo and M. Gan, 2011. Two-dimensional minimum local cross-entropy thresholding based on co-occurrence matrix. Comput. Electr. Eng., 37: 757-767.

Park, Y.K., S.L. Park and J.K. Kim, 2008. Retinex method based on adaptive smoothing for illumination invariant face recognition. Signal Process., 88: 1929-1945.

Sadr-Kazemi, N. and J.J. Cilliers, 1997. An image processing algorithm for measurement of flotation froth bubble size and shape distributions. Miner. Eng., 10: 1075-1083.

Wang, D., 1998. Unsupervised video segmentation based on watersheds and temporal tracking. IEEE Trans. Circuits Syst. Video Technol., 8: 539-546.

Wang, W., F. Bergholm and B. Yang, 2003. Froth delineation based on image classification. Miner. Eng., 16: 1183-1192.

Yang, C.H., J.Y. Yang, X.M. Mou, K.J. Zhou and W.H. Gui, 2008. A Segmentation method based on clustering pre-segmentation and high-low scale distance reconstruction for colour froth image. J. Electron. Inform. Technol., 30: 1286-1290.

Yang, C., C. Xu, W. Gui and K. Zhou, 2009. Application of highlight removal and multivariate image analysis to color measurement of flotation bubble images. Int. J. Imag. Syst. Technol., 19: 316-322.

Zhou, K.J., C.H. Yang, W.H. Gui and C.H. Xu, 2010. Clustering-driven watershed adaptive segmentation of bubble image. J. Cent. South Univ. Technol., 17: 1049-1057.